CO-PYROLYSIS OF SEWAGE SLUDGE AND MANURE

Nadia Ruiz-Gómez (nadiarui@unizar.es)[a], Violeta Quispe (vquispe@unizar.es)[a], Javier Ábrego (abrego@unizar.es)[a], María Atienza-Martínez (atienza@unizar.es)[a,*], María Benita Murillo (murillo@unizar.es)[a], Gloria Gea (glogea@unizar.es) [a]

[a]Thermochemical Processes Group (GPT), Aragon Institute for Engineering Research (I3A), Universidad Zaragoza, Spain

*Corresponding author:

Phone: + 34876555483 Fax: +34976762043

E-mail: atienza@unizar.es

ABSTRACT

The management and valorization of residual organic matter, such as sewage sludge and manure, is gaining interest because of the increasing volume of these residues, their localized generation and the related problems. The anaerobic digestion of mixtures of sewage sludge and manure could be performed due to the similarities between both residues. The purpose of this study is to evaluate the feasibility of the co-pyrolysis of sewage sludge (SS) and digested manure (DM) as a potential management technology for these residues. Pyrolysis of a sewage sludge/manure blend (50:50%) was performed at 525 ºC in a stirred batch reactor under N_2 atmosphere. The product yields and some characteristics of the product were analyzed and compared to the results obtained in the pyrolysis of pure residues. Potential synergetic and antagonist effects during the co-pyrolysis process were evaluated. Although sewage sludge and manure seem similar in nature, there are differences in their pyrolysis product properties and distribution due to their distinct ash and organic matter composition. For the co-pyrolysis of SS and DM, the

product yields did not show noticeable synergistic effects with the exception of the yields of organic compounds, being slightly higher than the predicted average, and the H_2 yield, being lower than expected. Co-pyrolysis of SS and DM could be a feasible management alternative for these residues in locations where both residues are generated, since the benefits and the drawbacks of the co-pyrolysis are similar to those of the pyrolysis of each residue.

KEYWORDS: sewage sludge; manure; co-pyrolysis; stirred batch reactor.

1. INTRODUCTION

The management and valorization of residual organic matter is a subject of growing interest because of the increasing volume of these residues, their localized generation and the associated environmental, economic and social issues. Sewage sludge and manure are two of the most abundant residues of this kind in Spain. The annual production of sewage sludge and livestock manure was 2.6 and 6 Mt (on a dry basis), respectively, in recent years in Spain (Eurostat, 2014). The residues are similar in nature, in terms of high water and nutrient (N and P) content. For this reason, one of the traditional disposal methods for both residues is land application. However, this practice is limited by environmental regulations and transportation costs. The improper application of these residues to fields, especially in those regions with high concentrations of intensive livestock production, provokes surface and groundwater pollution, odor and air emissions (ammonia and greenhouse gases), and the accumulation of heavy metals in soils. In the specific region of Aragón in Spain, only its capital is densely populated (Zaragoza, around 700,000 inhabitants). Rural areas around it are scarcely populated but some of them have a flourishing farming sector. As a result, around 82 kt/year of sewage sludge are generated, most of them in the area of Zaragoza. On the other hand, more than 11.5 and 2.3 Mt/year of pig and cattle manure are generated in Aragón. This quantity largely

exceeds the local demand for agricultural fertilizers (in terms of N content). Thus, at least a portion of these residues could be co-processed together with sewage sludge. This possibility is encouraged by the Integrated Waste Management Plan of Aragón (GIRA), which aims to achieve a better valorization of the residue flows within the region, while enabling the optimum operation of existing and new treatment plants. Moreover, integrated approaches are demanded for the valorization of residual organic matter such as sewage sludge, manure and/or municipal solid wastes. Therefore, the development of alternative technologies for the management of these kinds of residues is required. In this regard, the pyrolysis of anaerobically digested organic-based wastes appears as a potential method for valorizing these residues. This process stabilizes them, reduces their volume, and produces three product fractions (solid, liquid and gas) valuable for energy and/or chemical production.

The EU Framework Programme for Research and Innovation establishes the need for seeking innovative and sustainable technologies for the management of manure and other effluents from livestock production. A similar approach is applied to sewage sludge. The pyrolysis of each one of these residues has been investigated in the past; for instance, the pyrolysis of sewage sludge has been widely studied for liquid production (Fonts et al., 2012) and also for obtaining solid products that can be used as adsorbents (Smith et al., 2009). Most of the works on liquid obtained from sewage sludge pyrolysis have been focused on its application as a fuel, but its high nitrogen content hinders this usage. For this reason, more recently the use of sewage sludge pyrolysis liquid as a source of valuable chemicals has been investigated (Fonts et al., 2016). Regarding manure pyrolysis, most research works have been devoted to producing biochar for its application as a soil conditioner, showing several benefits as an organic amendment (Meng et al., 2013; Subedi et al., 2016). Studies on manure pyrolysis to produce bio-oil have been

sparse (Cao et al., 2011; Jeong et al., 2015) and mainly focused on poultry manure (Agblevor et al., 2010; Das et al., 2009), showing, as in the case of the bio-oil from sewage sludge, a relatively high nitrogen content compared to lignocellulosic biomass bio-oils.

Other authors have evaluated the co-pyrolysis of sewage sludge and lignocellulosic biomass in order to enhance the properties of the liquid for use as a fuel (Alvarez et al., 2015; Samanya et al., 2012) and to reduce the heat demand of the pyrolysis process (Ding and Jiang, 2013), proposing this co-pyrolysis as a viable solution for the valorization of sewage sludge (Alvarez et al., 2015) without external energy input (Ding and Jiang, 2013). The co-pyrolysis of manure with lignocellulosic biomass (Troy et al., 2013) and with agricultural plastic wastes (Ro et al., 2014) has also been evaluated with the aim of decreasing the energy requirements in the manure pyrolysis process without affecting the biochar properties.

Due to the similarities between sewage sludge and manure, the anaerobic digestion of their mixtures could be performed in locations where both residues are generated locally. Therefore, it would seem desirable to assess the co-pyrolysis of digested sewage sludge and manure with the aim of evaluating the feasibility of their joint valorization. However, the co-pyrolysis of both residues and its potential benefits has been scarcely studied (Sanchez et al., 2007). Sánchez et al. carried out a pilot-scale pyrolysis process for the treatment of a mixture of sewage sludge and cattle manure to evaluate the energetic valorization of the co-pyrolysis products, concluding that the co-pyrolysis products can be used as a fuel provided that the combustion gases are treated (Sanchez et al., 2007). In order to study the technical feasibility of co-pyrolizing these residues it would be necessary to assess the possible antagonist or the synergetic effects of the mixture of sewage sludge and manure on the pyrolysis product properties. However, these effects have barely been analyzed. Furthermore, it would be also interesting to assess the

89 economic feasibility of this process (Brown et al., 2013; Wright et al., 2010).

90 The purpose of this study is to compare the main properties of the pyrolysis products
91 obtained from digested sewage sludge (SS) and digested manure (DM) and to ascertain
92 the potential synergetic and antagonist effects during the co-pyrolysis process.

93 ## 2. MATERIALS AND METHODS

94 ### 2.1 Materials.

95 The anaerobically digested and thermally dried SS used for this work was supplied by
96 an urban wastewater treatment plant located in Madrid (Spain). The DM was supplied by
97 the HTN Biogas Company located in Navarra (Spain) and was obtained by anaerobic co-
98 digestion of cattle manure with food and agro-industry wastes. The anaerobically digested
99 manure was separated in a decanter centrifuge and the solid fraction was dried at 105 ºC.
100 The proximate and ultimate analysis, the higher heating value, the density and pH of these
101 materials contents are displayed in Table 1. The extractive content of both materials, also
102 shown in Table 1, was determined by Soxhlet extraction with dichloromethane. The
103 content of other organic macromolecules in SS and DM are also displayed in Table 1.

104 **Table 1.** Properties of the materials (wet basis).

Properties	Analytical standard	SS	DM
Ultimate analysis (wt. %)			
Carbon[a]		27.9	31.7
Hydrogen[a,b]		4.7	4.2
Nitrogen[a]		4.5	1.9
Sulfur[a]		1.4	0.5
Oxygen[c]		34.6	50.7
Proximate analysis (wt. %)			
Dry matter	ISO-589-1981	93	87
Ash	ISO-18122-2015	40	20
Volatiles	ISO-5623-1974	50	54
Fixed carbon[d]		3	13
Others			
HHV[e] ($MJ \cdot kg^{-1}$)	ISO-1928-2009	12.5	13.9
Density[f] ($kg \cdot m^{-3}$)		0.87	0.26
pH[g]		7.3	8.3
Extractives (wt. %)		3.5	1.0
Protein (wt. %)	EN-13342:2001	28	12
Neutral detergent fiber (NDF) (wt. %)	XP U44-162	26.78	49.54
Acid detergent fiber (ADF) (wt. %)	XP U44-162	4.26	46.77
Lignin (wt. %)	XP U44-162	0.03	16.34
NDF-ADF[h] (wt. %)		22.52	2.77

ADF-Lignin[i] (wt. %)		4.23	30.43

[a]Ultimate analysis was performed using Carlo Erba 1108. [b]The wt.% of hydrogen includes hydrogen from the moisture. [c]Oxygen (% wt) = 100-Carbon (%)-Hydrogen (%)-Nitrogen (%)-Sulfur (%)-other elements contained in the ash (%) (see Table 2). [d]By difference. [e]HHV was determined using IKA C 2000 Basic Calorimeter. [f]A known volume of material (25 mL) was weighed and the density was calculated. [g]1 g of solid is stirred for 1.5 h in demineralised water. [h]This fraction includes components such as hemicellulose. [i]This fraction includes components such as cellulose.

Compared to lignocellulosic biomass wastes, SS and DM have higher ash, nitrogen and sulfur contents. The lower ash content of DM (half of that from SS) explains the higher higher heating value (HHV) of this type of residue. The higher oxygen content for DM is not only due to its higher moisture content, but also to its organic chemical composition. This higher oxygen content justifies the lower HHV (if expressed in dry ash free basis) of DM than that of SS (20 vs. 23 $MJ \cdot kg^{-1}$). Another difference between both raw materials lies in their density, this being much lower for DM. Finally, the extractive and protein content was higher in SS than in DM. The extractives are the most non-polar compounds. The composition of the extractives was analyzed by Gas Chromatography and Mass Spectrometry (GC-MS). The compounds found in the extractives from SS were mainly fatty acids, toluene, benzene derivatives and steroids. The extractive compounds from DM were also fatty acids, toluene and phenolic compounds. DM contains larger amounts of lignin.

The high ash content in both materials could affect the pyrolysis process, since ash has been shown to have some catalytic effects (Aznar et al., 2007). The inorganic compounds found in the ash could increase the yield of char and non-condensable gases (NCG), and decrease the yield of liquid (Sekiguchi and Shafizadeh, 1984). According to Nik-Azar et al. (1997) Na and K have stronger catalytic effect than calcium. Table 2 displays the metal content of the wastes determined by Inductively Coupled Plasma-Atomic Emission

132 Spectroscopy (ICP-AES).

133 As can be seen in Table 2, calcium and iron are the most abundant metals in DM and

134 SS ash, respectively.

135 **Table 2.** Metal content of SS and DM.

Element	SS ($g \cdot kg^{-1}$)	DM ($g \cdot kg^{-1}$)
Al	21.75	9.04
As	<0.035	<0.035
Ba	0.333	0.024
Ca	22.99	55.4
Cd	<0.004	<0.004
Co	<0.007	<0.007
Cr	0.080	<0.065
Cu	0.41	<0.034
Fe	66.80	7.86
K	5.03	8.64
Mg	6.81	8.09
Mn	0.25	0.30
Mo	<0.165	<0.165
Ni	<0.021	<0.021
P	30.81	15.16
Pb	0.183	<0.133
Ti	1.5	<0.023
Zn	<0.026	0.33
Hg	<0.026	<0.026
Na	2.33	4.83
Si	48.8	0.39

136

137 Figure 1 shows the Fourier transform infrared (FTIR) spectra of both residues.

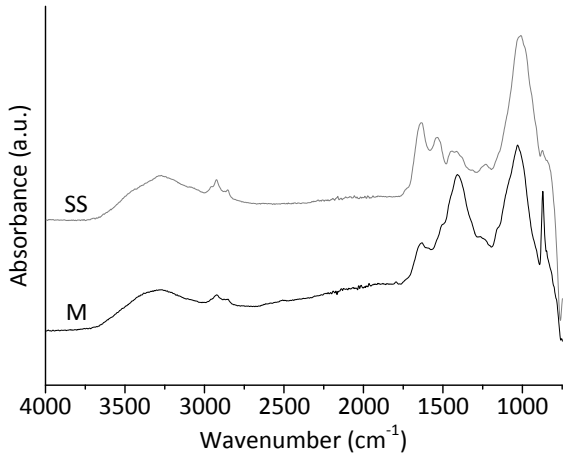

Figure 1. FTIR spectra of SS and DM.

In general, the SS used shows a similar spectrum to others previously reported (Abrego et al., 2009), the main differences (e.g. lower peak intensities) being attributable to the effect of the anaerobic digestion, which greatly reduces the intensity of some bands (Cuetos et al., 2013). The DM used in this work was also anaerobically digested and thus also exhibits broad bands with lower intensities. The comparison between both materials shows some similarities and several differences. Both of them show a band in the 1200-1000 cm^{-1} range attributed to polysaccharides. However, DM shows a distinctive band centered at 1409 cm^{-1} that could be explained by C=O stretching and OH deformation from carboxylic acids (Socrates, 2004). The presence of a higher number of these functional groups in DM could partly explain the higher O content of this material. On the other hand, the bands related to compounds with a protein origin (1790–1500 cm^{-1}) (Cuetos et al., 2013) are much more intense in the case of SS, which is in accordance with the higher N content of this material. The peak at 2800-3000 cm^{-1} indicates the presence of aromatic and aliphatic structures. The broad band between 3000-3700 cm^{-1} corresponds to the O-H stretching in water, alcohols, phenols and carboxylic acids, as well as N-H stretching from amides and amines (Alvarez et al., 2015). Finally, the very

high calcium content in DM could be evidenced by the sharp peak appearing in its spectrum at around 875 cm^{-1}, corresponding to calcium carbonate (Abrego et al., 2009). Another characteristic band for this compound appears at around 1420 cm^{-1} and could contribute to the previously mentioned band found at 1409 cm^{-1}.

As detailed in the next Section, both materials were pyrolyzed in the pyrolysis reactor without prior grinding. The particle size distributions for SS and DM are shown in Table 3.

Table 3. Particle size distribution for the raw materials.

Size (mm)	DM (wt. %)	SS (wt. %)
$\Phi > 4$	23	2
$3 < \Phi < 4$	9	54
$2 < \Phi < 3$	17	40
$0.8 < \Phi$ 2	30	2
$\Phi < 0.8$	21	2

2.2. Experimental system and procedure

Thermogravimetric analyses were performed prior to the pyrolysis runs in the stirred batch reactor. Both experimental systems are briefly described below.

2.2.1. Thermogravimetric analysis (TGA)

Thermogravimetric analyses were performed in order to study the thermal degradation behavior of each residue and of the 50:50% blend. A Netzsch STA 449 Jupiter® thermobalance was used. The two materials were ground and sieved to a particle size lower than 50 μm. The SS/DM blend (50%:50%) was prepared by blending both wastes, ground and sieved. The operating conditions used were the same for the three samples (SS, DM and SS/DM). The samples (ca. 20 mg) were heated up to 900 ºC at a heating rate of 10 $ºC \cdot min^{-1}$ under N_2 atmosphere (flow rate of 50 mL (STP)$\cdot min^{-1}$). Two replicates

were performed for each feedstock.

2.2.2. Pyrolysis tests in the stirred batch reactor.

A bench-scale stirred batch reactor was used to pyrolyze each residue alone (SS and DM) and also the 50:50% blend (SS/DM). Figure 2 illustrates the laboratory scale setup. The cylindrical reactor has a diameter of 107 mm and a length of 294 mm. The reactor capacity depends on the bulk density of the solid material fed. Since the bulk density of SS is higher, the amount of sample placed in the reactor was approximately 600 g for SS pyrolysis runs and around 300 g for DM and SS/DM runs. Four K-type thermocouples were used to register the temperature profiles in the reactor. The pyrolysis experiments were performed under N_2 atmosphere (250 mL (STP)·min^{-1}) at 525 ºC as the final temperature and at a heating rate of around 8 ºC·min^{-1} (this was the maximum heating rate achievable by the experimental system). The final temperature was maintained for 30 min. The vapors produced during the pyrolysis process passed through the condensing zone. The condensable fraction (water and organic compounds) was collected in two ice-cooled condensers and one electrostatic precipitator. The composition of NCG was analyzed by a micro-gas chromatograph (micro-GC) connected online. Specifically, the analyzed gases were CO_2, CO, H_2, CH_4, C_2H_2, C_2H_4, C_2H_6 and H_2S. The experiments were conducted in duplicate.

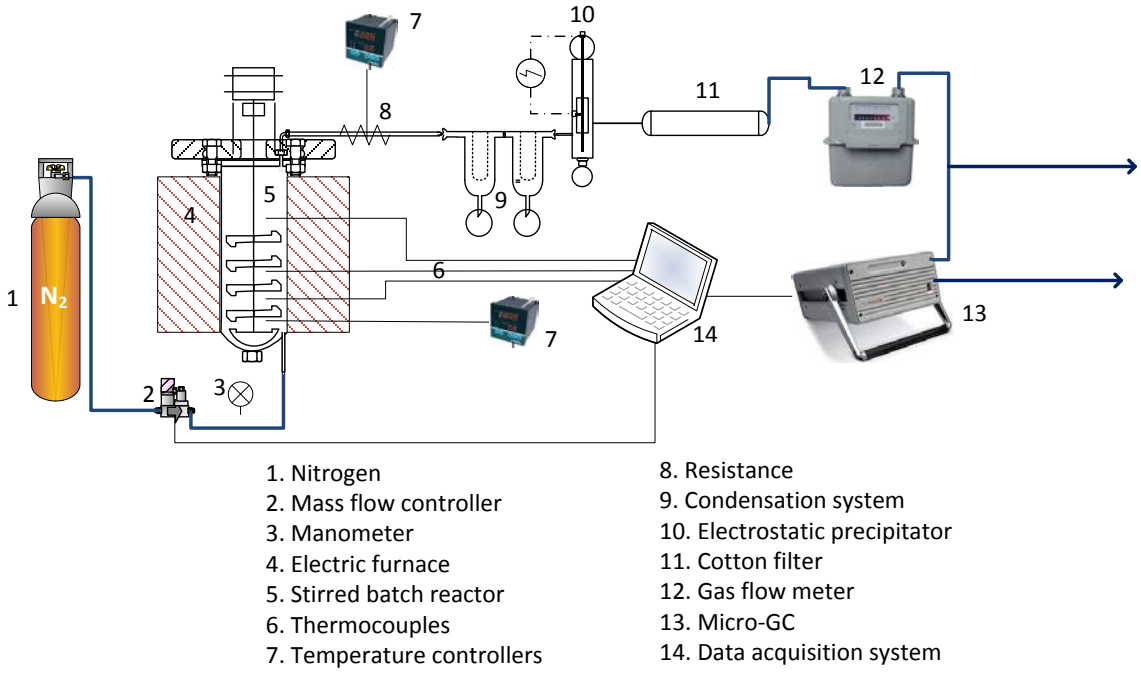

Figure 2. Laboratory scale pyrolysis setup.

2.2.3 Characterization of pyrolysis products

The mass yields of each one of the pyrolysis products ($\eta_{product}$) were calculated as the percentage ratio between the mass of pyrolysis product and the mass of feedstock introduced into the reactor. The mass of solid (char) and liquid obtained was determined gravimetrically. The mass of gas obtained was calculated taking into account the gas composition provided by the micro-GC and the known volumetric flow of nitrogen introduced.

The lower heating value of the gas (free of N_2) (LHV_{gas}) was calculated considering the gas composition and the lower heating value of each gas compound. The ultimate and proximate analyses and the higher heating value of the char (HHV_{char}) obtained in each experiment were determined. The FTIR analysis of the char was also performed and the results were compared to the FTIR spectra of the different residues.

The liquid, which separated into two phases (aqueous phase (AP) and organic phase (OP)) in all the experiments performed, was centrifuged at 4500 rpm (2038 x g) for 30 min using a Heraeus Megafuge 16 Centrifuge to separate both phases. The phases were stored in a fridge at between 3 °C and 5 °C until they were analyzed. The water content (WC, mass fraction %) of each phase was determined by the Karl-Fischer titration method. The density of both phases was determined using a portable Mettler Toledo densimeter (model Densito 30 PX). The ultimate analysis and the higher heating value of the organic phase (HHV_{OP}) were also measured. The organic compounds present in both phases were identified and semi-quantified by GC-MS and GC-FID. The chromatographic methods used for both phases showed certain differences. The capillary column used for analyzing the aqueous phases was a 50 m x 200 μm x 0.3 μm HP-FFAP Polyethylene Glycol TP. Helium of 99.999% purity was used as the carrier gas and the injector temperature was set at 300 ºC. The temperature program adopted was the following: initial oven temperature at 60 ºC held for 6 min followed by an increase to 80 ºC at a rate of 1.5 ºC·min^{-1} and held for 5 min, consequently increased to 200 ºC at a rate of 1 ºC·min^{-1} and held for 5 min, and finally increased to 240 ºC at a rate of 1.8 ºC min^{-1} where it was held for 30 min. The capillary column used for the organic phases was 60 m x 250 μm x 0.25 μm DB-17ms. The carrier gas and the injector temperature were similar to those used for the aqueous phases. The temperature program was as follows: initial oven temperature at 60 ºC held for 5 min followed by an increase to 250 ºC at a rate of 1.5 ºC min^{-1} and held for 5 min, and finally an increase to 310 ºC at a rate of 2 ºC·min^{-1} and held for 5 min. The analysis procedure used considers all the response factors to be similar. It therefore does not give quantitative results but is suitable for comparing relative percentages of compounds in pyrolysis liquids.

The energy yield of the different products, defined according to equation [1], was

235 calculated for each run.

236 $$energy\ yield_i = \frac{\eta_i HHV_i}{HHV} \times 100 \quad [1]$$

237 where η_i and HHV_i are the mass yield and the higher heating value of each pyrolysis
238 product (gas, organic liquid phase and char, respectively) and HHV is the higher heating
239 value of the material introduced into the reactor (or the average of HHVs in the case of
240 SS/DM).

241 Finally, the energy requirement for the pyrolysis process was estimated for each waste
242 and the blend. The procedure followed to solve the energy balances was similar to those
243 used by other researchers (Abrego et al., 2013; Atienza-Martinez et al., 2015; Gil-
244 Lalaguna et al., 2014).

245

246 ## 3. RESULTS AND DISCUSSION

247 ### 3.1 TGA experiments

248 The mass loss (TG) and derivative mass loss (DTG) curves are displayed in Figure 3.
249 Both materials show total mass loss greater than 50% at the final temperature of 900 ºC
250 and a main decomposition stage in the temperature interval between 200 and 400 ºC. This
251 stage begins slightly later for DM than for SS (DTG peaks at 325 ºC and 310 ºC,
252 respectively) which could be explained by the higher cellulose content in DM.
253 Immediately after this main decomposition stage, SS shows additional mass loss
254 evidenced by a shoulder in its DTG curve, which can be associated with protein
255 decomposition. The region between 500 and 650 ºC is quite similar for both materials,
256 with relatively constant mass loss. Major differences arise at higher temperatures, with
257 more significant mass loss for DM peaking at 715 ºC. This peak may be attributed to

calcium carbonate decomposition (Abrego et al., 2009). This compound has been identified in the FTIR spectrum of DM (Figure 1). Furthermore, calcium is the most abundant component of the DM ashes, and the manure pH, higher than 7, indicates a significant proportion of carbonates in the ashes (Schumacher, 2002).

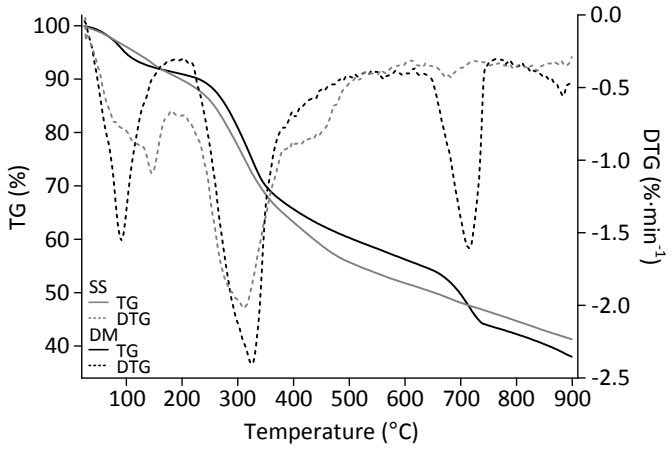

Figure 3. Mass loss (TG) and derivative mass loss (DTG) curves for SS and DM.

The experimental and the predicted (arithmetic average from the results obtained for each material) DTG curves for SS/DM are compared in Figure 4 in order to assess potential synergistic effects. In order to better compare the main decomposition features, the drying region, below 100 ºC, is not shown in the figure. The predicted and the experimental curves were quite similar. The region below 500 ºC was almost identical, with a minor difference in the DTG peak maximum (the predicted curve showed a DTG peak maximum at 318.5 ºC, whereas the experimental curve gave 312.5 ºC). At higher temperatures, experimental data showed lower mass loss than predicted, especially from 700 ºC. It seems that the carbonate decomposition region already shown for DM in Figure 3 was affected in two ways by the presence of SS. On the one hand, the experimental DTG temperature peak was 698.5 ºC vs. the predicted peak at 713.5 ºC. On the other hand, the total mass loss in this stage was lower than the arithmetic average of both

277 contributions.

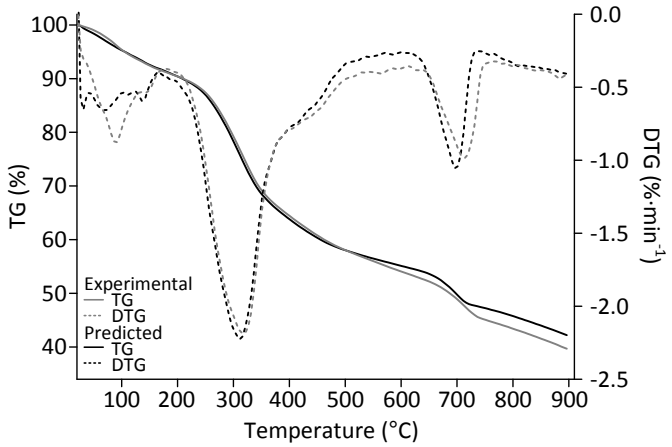

278

279 **Figure 4**. Experimental and predicted TG and DTG curves for SS/DM blend.

280

281 3.2 Product yields in the stirred batch reactor

282 Mass balance closure was higher than 90% for all the experiments performed.
283 Pyrolysis product yields from the pyrolysis of each residue and from the co-pyrolysis of
284 both are displayed in Figure 5. The predicted average yields are also shown in Figure 5.

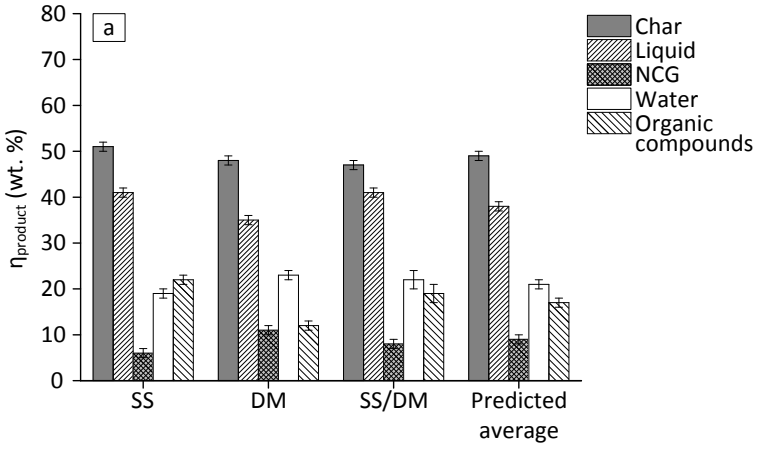

285

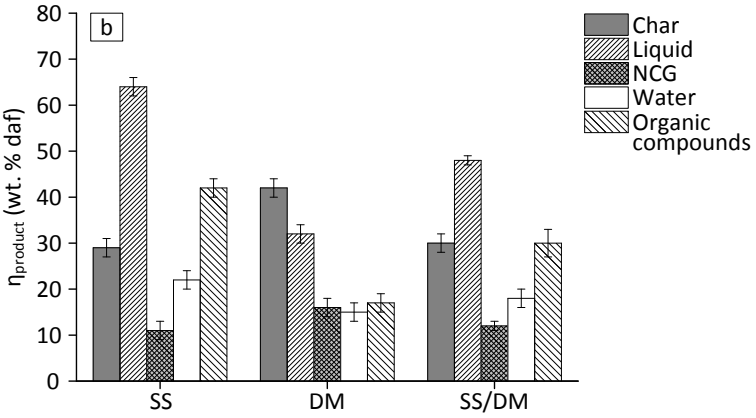

286

287 **Figure 5**. a) Product yields, expressed on feedstock basis, from the pyrolysis of SS,
288 DM and SS/DM b) Product yields, expressed on a dry ash free basis, from the pyrolysis
289 of SS, DM and SS/DM.

290

291 Although sewage sludge and manure are not very different in nature, their pyrolysis
292 product distribution showed certain differences. The pyrolysis of DM produced a higher
293 gas yield, and lower char and liquid yields than the pyrolysis of SS (Figure 5a). The higher
294 ash content of SS explains its higher char yield. However, if expressed on a dry ash free
295 basis, the char yield from the DM pyrolysis is higher than that from SS (see Figure 5b).
296 These results are in accordance with the higher fixed carbon content of the DM (see Table
297 1), which could be justified by its higher lignin content and lower extractives content. It
298 is known that the char yield from the pyrolysis of lignin is high (Qu et al., 2011) whereas
299 the char yield from the pyrolysis of lipids or extractives is low. Sewage sludge contains a
300 higher proportion of proteins and the char from the pyrolysis of proteins is also high
301 (Kebelmann et al., 2013), but not as high as that from lignin. The higher gas yield from
302 the pyrolysis of DM could be attributed to the catalytic activity of the metals present in
303 the ash (Manya et al., 2006). DM contains higher concentrations of Ca and Na than SS
304 (5.5% and 0.5% for Ca and Na in DM vs. 2.3% and 0.2%, respectively, in SS). These

305 species would promote the degradation of the organic matter, favoring the gas formation
306 (Zabeti et al., 2012). The higher moisture content of DM could explain the higher water
307 yield from the pyrolysis of DM. However, the water yield expressed on dry ash free basis
308 was lower using DM as the feedstock (see Figure 5b). The water generated by the
309 pyrolysis reactions was higher in the case of the SS pyrolysis. The higher H/O molar ratio
310 in SS (H/O = 2.2 for SS vs. H/O = 1.1 for DM, expressed on dry basis) makes it possible
311 that a greater amount of the organic oxygen present in the starting material may be
312 converted into water during the pyrolysis process (Mullen and Boateng, 2011). Other
313 authors have observed that the pyrolysis of biomass with high protein content results in
314 higher water production because of the reaction of nucleophilic amine groups with
315 electrophilic oxygen groups releasing water (Mullen and Boateng, 2011). The DM used
316 in this study has lower protein content than the SS, which could produce lower amounts
317 of pyrolytic water and consequently a lower water yield, expressed on dry ash free basis.
318 The amount of condensable organic compounds generated by pyrolysis was much lower
319 for DM. DM has a lower amount of extractives than SS. Lipids generate a high level of
320 volatiles (Kebelmann et al., 2013) which could explain the higher organic compound
321 yield from SS. Furthermore, the presence of a higher content of some alkali metals such
322 as Ca and Na in DM could also provoke a reduction in the yield of organic compounds,
323 promoting the gas yield (Zabeti et al., 2012).

324 For the co-pyrolysis of SS and DM, the product yields showed an expected behavior,
325 i.e. there were no noticeable synergistic effects, with the exception of the yield of organic
326 compounds. The product yields obtained from the pyrolysis of the blend of SS and DM
327 was approximately the average of the yields obtained from each individual residue
328 (Figure 5a). However, the yield of organic compounds obtained from the pyrolysis of the
329 SS/DM blend was slightly higher than the predicted average. This might be attributed to

330 the reduction in the alkali metal content in the SS/DM blend feedstock compared to DM,
331 causing the secondary reactions to occur to a lesser extent. Other authors have observed
332 important synergies in the co-pyrolysis of sewage sludge and different types of
333 lignocellulosic biomass, such as poplar sawdust (Zuo et al., 2014), rice husk (Zhang et
334 al., 2015) and sawdust(Alvarez et al., 2015), which they have attributed to the catalytic
335 activity of the ash present in the sewage sludge. The synergy resulted in increasing gas
336 yields and decreasing bio-oil yields. The more similar ash content in SS and DM in
337 comparison with lignocellulosic biomass could explain the lesser synergistic effect on the
338 product yields between the two materials studied in this work.

339 3.3. Gas characterization

340 The yields of NCG obtained from the pyrolysis of each residue and the co-pyrolysis
341 are displayed in Figures 6a and 6b. The major gas compound in all the experiments was
342 CO_2. The pyrolysis of SS produced lower yields of CO_2 and CO and higher yields of H_2
343 and H_2S than the DM pyrolysis. CO_2 and CO derived from decarboxylation and
344 decarbonylation reactions, respectively. The higher proportion of carbonyl and carboxyl
345 groups in DM enhanced the formation of both CO_2 and CO. Furthermore, Na and Ca,
346 which are present in higher proportions in DM, are active catalysts for generating CO_2
347 and CO during pyrolysis (Zabeti et al., 2012). The higher molar ratio H/C in SS (1.6 for
348 SS vs. 0.9 for DM, expressed on dry basis), together with the higher content of Al_2O_3 in
349 the SS ashes which might promote H_2 production (Azuara et al., 2013), could explain the
350 higher H_2 yield in the SS pyrolysis. Furthermore, the higher lignin content in DM
351 disfavors H_2 production, since lignin devolatilization generates less H_2 than other
352 chemical constituents, such as cellulose or hemicellulose (Li et al., 2004). The lower H_2S
353 yield from the pyrolysis of DM could be explained by the lower S content in this material.
354 As can be seen from Figure 6, no relevant synergistic effects regarding the gaseous

products were found when pyrolyzing SS/DM, with the exception of H_2. The yield of H_2 from the co-pyrolysis was lower than that calculated as the predicted average. This antagonist effect might be attributed to the reduction in the Al content in the SS/DM blend feedstock compared to SS.

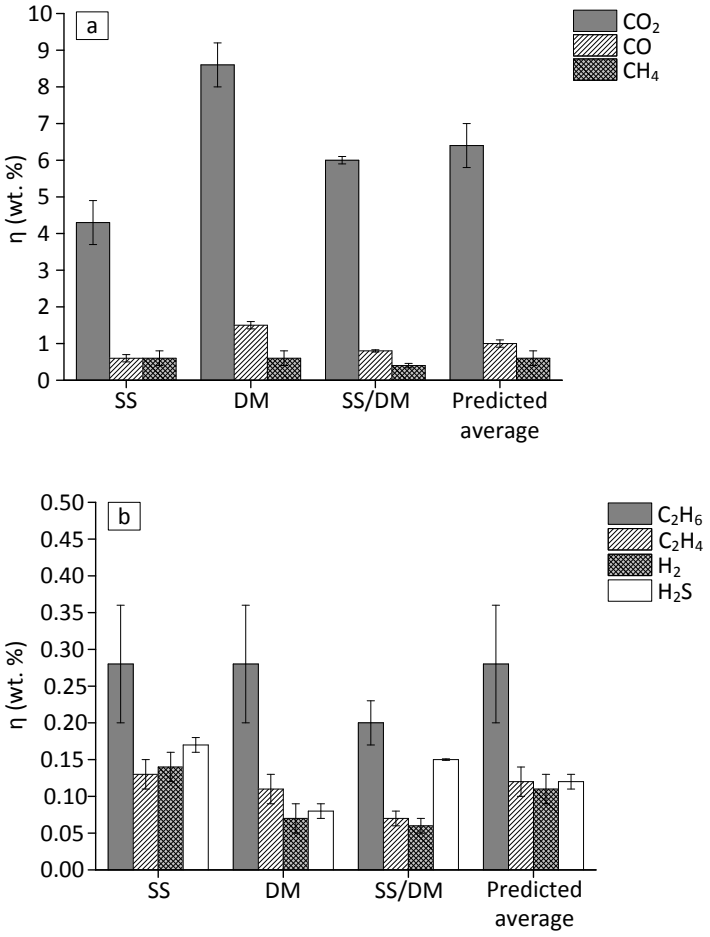

Figure 6. NCG yields from the pyrolysis of SS, DM and SS/DM blend a) CO_2, CO, and CH_4 yields, b) H_2, H_2S, C_2H_4, and C_2H_6 yields.

According to the gas composition, the LHV_{gas} (N_2 free) from the DM pyrolysis (6 ± 1 MJ·m$^{-3}_{STP}$) was lower than that from the SS pyrolysis (10 ± 1 MJ·m$^{-3}_{STP}$). The LHV_{gas} from the SS/DM co-pyrolysis (6 ± 1 MJ·m$^{-3}_{STP}$) was similar to the LHV_{gas} from DM and lower than predicted average value (8 ± 1 MJ·m$^{-3}_{STP}$) since, as already indicated, the H_2 yield is also lower. In any case, the LHV of the NCG produced from the three

types of feedstock could be enough to use the gas as a fuel, although a system for cleaning combustion gases would be required.

3.4. Liquid characterization

The liquid product obtained from the pyrolysis of each residue is heterogeneous, showing two different phases (AP and OP, as stated in the Experimental Section). The AP was the major liquid phase in all the runs (Table 4). The OP yield was much lower from the DM than from the SS pyrolysis. However, the AP yield was similar for all the runs (Table 4). The OP yield obtained from the co-pyrolysis seemed to increase slightly more than the amount explainable by a predicted average, as was the case with the yield of organic compounds. Water was the major component present in the liquid. Table 4 shows the water content of the liquid phases obtained. The OP from the DM pyrolysis and from the co-pyrolysis showed a higher water proportion than the OP obtained from the SS pyrolysis. More polar organic compounds can be expected in the OP from the DM pyrolysis.

Table 4. Liquid phase yields (expressed on a feedstock basis) and water content. The values are expressed as mean ± standard deviation

Feedstock	Liquid phase yields (wt. %)		Water content (wt. %)	
	OP	AP	OP	AP
SS	13 ± 1	28 ± 1	7 ± 2	63 ± 1
DM	5.5 ± 0.5	29.8 ± 0.5	17 ± 6	75 ± 1
SS/DM	11 ± 1	29 ± 1	15 ± 5	68 ± 2
Predicted average	9 ± 1	29 ± 1	12 ± 6	69 ± 1

As shown in Table 5, the HHV of the organic phases obtained from each residue reflected the potential of these fractions for their use as liquid fuels. However, their nitrogen and sulfur contents, which are relatively high, hinder this application, since their combustion may lead to NOx and SOx generation. The N content in the organic phase

390 from the pyrolysis of DM was lower than that of the OP from the pyrolysis of SS because
391 the N content in SS is higher. Nevertheless, the application of these OPs as a source of
392 valuable chemical products, such as N-containing compounds (amides, imidazoles and
393 pyridines, among others), could represent an opportunity for SS and DM, since there are
394 not too many renewable sources for these types of compound (Fonts et al., 2016). No
395 noticeable synergistic effects were reflected for the SS/DM blend in either the ultimate
396 analysis or the H/C and O/C molar ratios.

Table 5. Ultimate analysis (dry basis), molar ratios H/C and O/C (dry basis), and higher heating value of the organic phases (wet basis). The values are expressed as mean ± standard deviation

	SS	DM	SS/DM	Predicted average
Carbon (wt. %)	69 ± 1	69 ±5	65 ± 8	69 ± 5
Hydrogen (wt. %)	9 ± 0.2	7.2 ± 0.4	7 ± 2	8.0 ± 0.4
Nitrogen (wt. %)	8.3 ± 0.2	4.9 ± 0.2	6.9 ± 0.4	6.6 ± 0.2
Sulfur (wt. %)	1.9 ± 0.2	1.4 ± 0.3	1.9 ±0.5	1.7 ± 0.3
Oxygen (wt. %)[a]	12 ± 1	18 ± 5	19 ± 8	15 ± 5
H/C	1.6	1.3	1.3	1.4
O/C	0.1	0.2	0.2	0.2
HHV (MJ kg^{-1})	34 ± 2	29 ± 2	29 ± 4	32 ± 2

[a]Calculated by difference.

Table 6 shows the ultimate analyses of the aqueous phases and the pH of these phases. As can be observed, the pH of the AP from the DM pyrolysis was lower than that of the SS pyrolysis.

405 **Table 6.** Ultimate analysis (dry basis) and pH for the aqueous phases. The values are
406 expressed as mean ± standard deviation

	SS	DM	SS/DM	Predicted average
Carbon (wt. %)	27 ± 1	23 ± 1	24 ± 1	25 ± 1
Hydrogen (wt. %)	7.2 ± 0.3	7.6 ± 0.2	6.6 ± 0.4	7.4 ± 0.2
Nitrogen (wt. %)	16 ± 1	6 ± 1	11 ± 2	11 ± 1
Sulfur (wt. %)	1.2 ± 0.1	0.43 ± 0.05	0.69 ± 0.03	0.8 ± 0.1
pH	9.5 ± 0.5	6 ± 1	8.7 ± 0.2	8 ± 1

407

408 3.4.1 Composition of the organic phases

409 The organic compounds identified by GC-MS in the OP have been grouped into
410 chemical families. The area percentage of each family identified is shown in Figure 7.

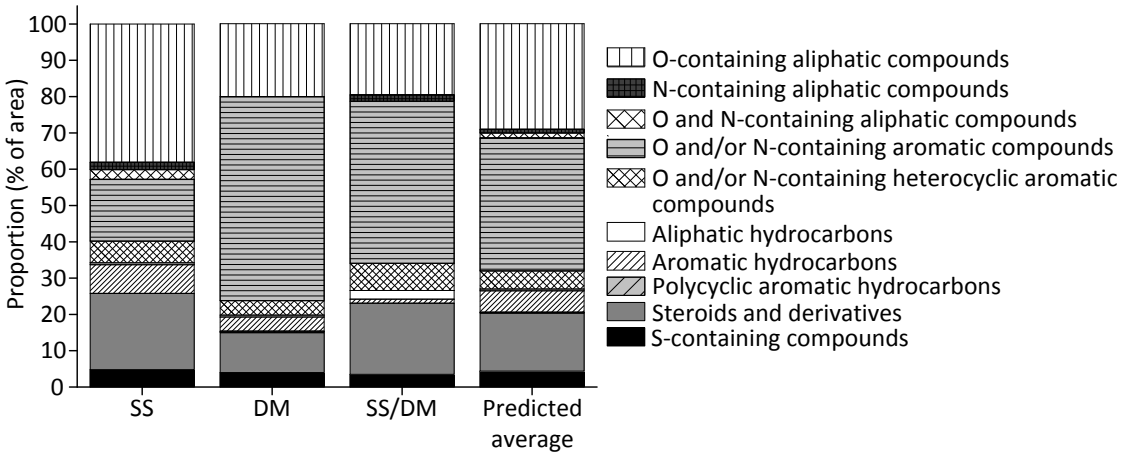

411

412 **Figure 7**. Composition of the OP obtained from the pyrolysis of SS, DM and SS/DM.

413

414 Table 7 shows the chromatographic area percentages of certain organic compounds
415 identified in the organic phase obtained in the co-pyrolysis of SS and DM, and of those
416 derived from the pyrolysis of each material independently.

417 **Table 7**. Chromatographic area percentage of certain organic compounds identified in the
418 OP obtained from the pyrolysis of SS, DM and SS/DM blend.

	SS (%)	DM (%)	SS/DM (%)
Carboxylic acids	31.8	13.0	10.7
Alcohols	1.3	3.2	2.5
Nitriles	3.2	0.0	2.9
Phenols	10.0	31.9	31.1
Cholestenes	12.2	1.3	8.4

419

420

421 Oxygen-containing aliphatic compounds (mainly carboxylic acids), as well as steroids
422 and their derivatives, were the main compounds in the OP from the pyrolysis of SS.
423 However, the main organic compounds from the pyrolysis of DM were nitrogen and/or
424 oxygen-containing aromatic compounds (mainly phenols). Fatty acids stem from their
425 direct devolatilization from SS and DM, since the extractives of both residues also contain
426 these compounds. The lower extractives content in DM could explain the lower
427 proportion of steroids in the organic phase from DM. The OP from the pyrolysis of DM
428 exhibited a lower proportion of non-polar compounds, which could justify its higher
429 water content. Phenols, more abundant in the OP from the pyrolysis of DM, could come
430 from lignin and protein decomposition. DM is characterized by its lignin and protein
431 content, which could generate phenolic compounds during pyrolysis (especially lignin)
432 (Amen-Chen et al., 2001; Parnaudeau and Dignac, 2007). The greater lignin content of
433 DM could explain the greater proportion of phenols in the OP from the pyrolysis of this
434 residue than in the OP from the pyrolysis of SS. Furthermore, it is noteworthy that no
435 nitrogen-containing aliphatic compounds (such as nitriles) were present in the OP from
436 the pyrolysis of DM. Aliphatic nitriles come from the reaction between fatty acids and
437 ammonia, both produced during pyrolysis. Not enough fatty acids and/or ammonia were

438 generated during the DM pyrolysis to generate aliphatic nitriles. However, the proportion
439 of fatty acids decreased and the proportion of aliphatic nitriles increased in the OP from
440 the pyrolysis of the SS/DM blend in comparison to the predicted average proportions.
441 This could be provoked by the reaction of the fatty acids from the DM pyrolysis with the
442 ammonia from the SS pyrolysis.

443 3.4.2. Composition of the aqueous phases

444 The organic compounds identified in the AP by GC-MS have been grouped into the
445 chemical families whose area percentages are shown in Figure 8.

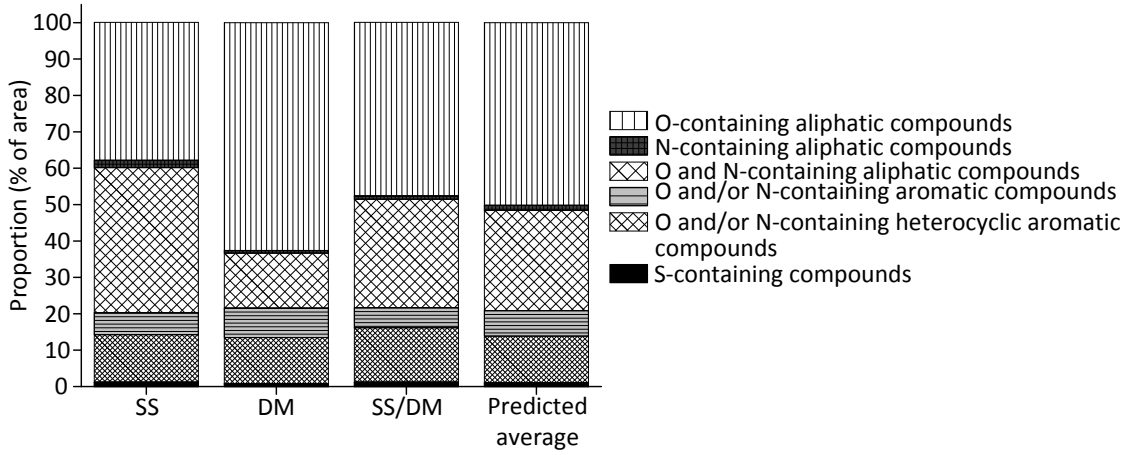

446

447 **Figure 8**. Composition of the AP obtained from the pyrolysis of SS, DM and SS/DM
448 blend.

449

450 The area percentages of the different chemical families present in the AP from the
451 pyrolysis of the SS/DM blend were similar to the predicted averages. In this regard, the
452 synergistic effects were less pronounced on the AP than on the OP.

453 Table 8 shows the chromatographic area percentages of certain organic compounds
454 identified in the aqueous phases.

455 **Table 8.** Chromatographic area percentages of certain organic compounds identified in
456 the AP from the pyrolysis of SS, DM and SS/DM blend.

	SS (%)	DM (%)	SS/DM (%)
Carboxylic acids	35.6	34.0	38.9
Alcohols	0.5	6.2	2.1
Ketones	0.4	8.7	1.7
Lactones	0.0	4.7	1.4
Amides	19.0	4.7	13.5
Furans	0.0	4.3	2.2
Pyrroles	9.1	4.1	5.8
Imidazoles	7.5	1.3	7.1
Phenols	1.7	7.5	3.5
Pyridines	7.2	5.3	7.1
Pyrazines	0.0	2.1	3.8

457

458 Oxygen and nitrogen-containing aliphatic compounds, mainly amides, and oxygen-
459 containing aliphatic compounds, mainly carboxylic acids, were the most abundant
460 families in the AP from the pyrolysis of SS. In the case of DM, carboxylic acids were by
461 far the major organic compounds. Alcohols, ketones and lactones were also significant in
462 the AP from the pyrolysis of DM, which would come from the devolatilization of
463 cellulose or other polysaccharides in the DM (Parnaudeau and Dignac, 2007). Acetic acid
464 was the organic compound found in the greatest proportion in the AP obtained from each
465 individual residue and from the SS/DM blend, being more abundant in the AP from the
466 pyrolysis of DM. This could explain its lower pH. Acetic acid comes from the elimination
467 of acetyl groups present in polysaccharides (Prins et al., 2006), such as cellulose, which
468 are more abundant in DM than in SS. The higher content in polysaccharides of DM could
469 also explain the higher proportion of furans (Parnaudeau and Dignac, 2007) in the AP
470 from the pyrolysis of this residue than that of SS. Again, the greater proportion of phenols
471 in the AP from the pyrolysis of DM than that of SS could be attributed to the higher lignin
472 content of DM. The total proportion of oxygen and/or nitrogen-containing heterocyclic
473 aromatic compounds, mainly pyridines, pyrazines, pyrroles and imidazoles, was similar

for both materials. Pyridines and pyrazines could come from nucleic acids and amino acids with heteroatomic rings (Fullana et al., 2003). Pyridines, which could come from proteins which contain aniline, were more abundant in the AP from the pyrolysis of SS. Pyrazines, which could also derive from the Maillard reaction which involves the formation of N-heterocycles by amino acids interacting with sugars (Schnitzer et al., 2007), were only present in the AP from DM. The higher proportion of pyrroles (Tsuge and Matsubara, 1985) and imidazoles in the AP from the pyrolysis of SS was also related to the higher protein content in this residue compared to DM. Acetamide, which could come from the pyrolysis of labile proteins that contain glycine (Parnaudeau and Dignac, 2007; Zhang et al., 2013) or from cell wall amino sugars(Eudy et al., 1985), was present in a higher proportion in the AP from the pyrolysis of SS, due to the higher content of proteins in SS. This could contribute to the increase of the pH of the AP from the SS pyrolysis.

3.5. Char characterization

The properties of the chars obtained from the different pyrolysis runs are summarized in Table 9.

490 **Table 9**. Properties of the chars obtained from the pyrolysis of SS, DM and SS/DM blend.
491 The values are expressed as mean ± standard deviation

Properties	SS	DM	SS/DM	Predicted average
Ultimate analysis (wt. %)				
Carbon	20 ± 2	42 ± 2	30 ± 0.4	31 ± 2
Nitrogen	2.5 ± 0.1	1.8 ± 0.1	2.38 ± 0.03	2.2 ± 0.1
Hydrogen	0.94 ± 0.06	1.51 ± 0.04	1.18 ± 0.08	1.23 ± 0.06
Sulfur	1.3 ± 0.1	0.89 ± 0.01	0.9 ± 0.2	1.1 ± 0.1
Proximate analysis (wt. %)				
Volatile matter	20.2 ± 0.5	20.2 ± 0.9	19.5 ± 0.1	20.2 ± 0.9
Fixed carbon	5.7 ± 0.5	37 ± 1	18.2 ± 0.4	21 ± 1
Ash	74 ± 1	42 ± 1	62.2 ± 0.3	58 ± 1
HHV ($MJ \cdot kg^{-1}$)	8 ± 1	14 ± 2	11 ± 1	10 ± 3

492

493 The char obtained from the DM pyrolysis exhibited, in principle, better characteristics
494 for energetic applications than that from the SS pyrolysis: the ash content was lower and
495 the fixed carbon content was higher in the DM char than in the SS char, which led to a
496 higher calorific value in the former. Furthermore, the content of nitrogen and sulfur,
497 which act as contaminants in a fuel, were lower in the DM char. Nevertheless, the ash,
498 nitrogen and sulfur contents of the DM char were still high in comparison with chars from
499 other types of biomass, such as lignocellulosic ones. The char obtained from SS/DM co-
500 pyrolysis shows no significant interactions between SS and DM. The uses of the char

obtained from the co-pyrolysis could be similar to those proposed for the char from the pyrolysis of each individual residue, such as adsorbent solids and soil amendments. However, the potential application of the char as soil amendment should be corroborated from an agronomic point of view.

Figure 9 shows the FTIR results from the char obtained from the pyrolysis of DM, SS and SS/DM blend.

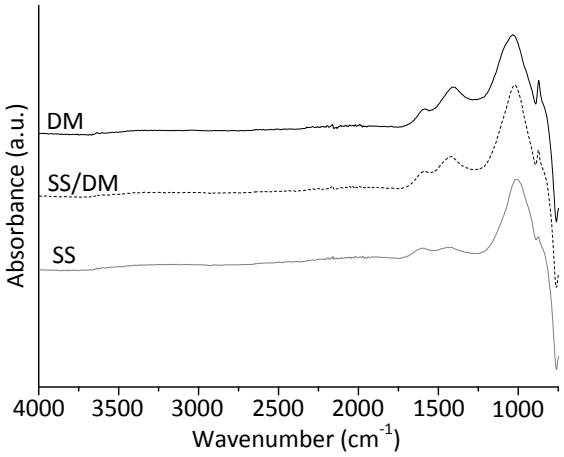

Figure 9. FTIR spectra of SS, DM and SS/DM chars.

A comparison with the FTIR spectra of the starting materials (shown in Figure 1) shows that pyrolysis causes the reduction or even disappearance of most of the previously identified peak regions. This can be correlated with some of the findings reported in the sections describing the composition of the OP and AP liquid fractions. In particular, the abundance of N-containing compounds, alcohols, phenols and fatty acids in the liquids might account for the absence of the previously identified N-H and O-H stretching (3000-3700 cm^{-1}) and protein band (1500-1790cm^{-1}), whereas the reduction of the C=O stretching (1409 cm^{-1}) in the case of DM could lead to the formation of oxygenated compounds such as ketones, abundant in the AP from this material. SS/DM chars still

519 show the presence of calcium carbonate inherited from DM.

520 3.6. Energy analysis

521 The energy yields of the products, based on HHV, indicate the percentage of the initial
522 energy content of the residue contained in each pyrolysis product. Table 10 displays the
523 energy yield results.

Table 10. Energy yields of the products. The values are expressed as mean ± standard deviation

	SS (%)	DM (%)	SS/DM (%)	Predicted average (%)
NCG	6 ± 1	6 ± 2	4 ± 1	6 ± 2
OP	35 ± 2	12 ± 2	24 ± 2	23 ± 2
Char	33 ± 1	49 ± 5	40 ± 1	41 ± 5
Total	74 ± 2	67 ± 5	68 ± 2	70 ± 5

The total energy yield in the case of the SS pyrolysis was higher than that obtained for the pyrolysis of DM, mainly due to the lower energy recovery of the OP.

The energy balances were calculated for the system shown in Figure 10 to compare the energy requirements for the pyrolysis of each individual residue and for the SS/DM blend.

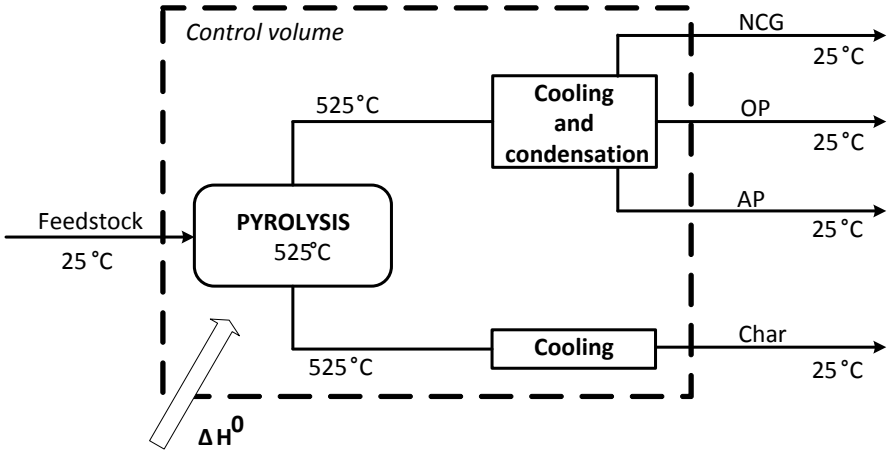

Figure 10. Energy balance system for pyrolysis of SS, DM and SS/DM. Reference temperature: 25 °C. Reference pressure: $1.01 \cdot 10^5$ Pa.

The different feedstocks and the pyrolysis products have been considered to be at the reference conditions of pressure and temperature (25 °C and $1.01 \cdot 10^5$ Pa). This means

537 that the energy released from the cooling of the char and the NCG, and from the cooling
538 and the condensation of the condensable vapors, was completely used. Assuming no heat
539 losses in the system, the input energy (H_{input}) included the feedstock chemical energy. The
540 output energy (H_{output}) included the chemical energy of all the products. The chemical
541 energy of the feedstocks, the char and the OP has been calculated from their ultimate
542 analyses and their HHVs. In the case of the AP, the chemical energy has been determined
543 assuming that these phases were a blend of water and acetic acid, which was the most
544 abundant organic component in the aqueous phases.
545 Taking into account the aforementioned simplifications, the ΔH^0, calculated using
546 equation [2], indicates the energy requirement of the process (per kg of feedstock).

547 $$\Delta H^0 = H_{output} - H_{input} = \frac{\sum_i \eta_i \cdot \Delta H^0_{f,i}}{100} - \Delta H^0_{f,feedstock} \quad [2]$$

548 where η_i is the yield of each product, $\Delta H^0_{f,i}$ the apparent enthalpy of formation of each
549 product and $\Delta H^0_{f,feedstock}$ the apparent enthalpy of formation of the feedstock.
550 The ΔH^0 has been calculated for each one of the pyrolysis runs. The results are
551 presented in Table 11.
552 **Table 11**. ΔH^0 obtained for pyrolysis of SS, DM and SS/DM. The values are expressed
553 as mean ± standard deviation

	ΔH^0 (MJ·kg^{-1})
SS	-0.6 ± 0.1
DM	-4.2 ± 0.8
SS/DM	-2.1 ± 0.1
Predicted average	-2.4 ± 0.1

554
555 All the values obtained for ΔH^0 were negative which theoretically means that in the
556 absence of heat losses, the energy that could be used from the cooling and condensation

of the products was higher than the energy required for the process. In these terms, the DM pyrolysis and co-pyrolysis of both residues showed much more exothermic behavior than the SS pyrolysis.

However, the energy required for the drying of both residues should also be considered. The heat required to reduce the water content of the residues from 65% (typical minimum humidity value obtained from a mechanical dehydration system) to 7-10%, which is recommended for the pyrolysis process, was approximately 4 $MJ \cdot kg^{-1}$ of dried residue (Gil-Lalaguna et al., 2014). Therefore, it is important to efficiently use the energy for the cooling and condensation of the pyrolysis products from an energetic point of view.

4. CONCLUSIONS

The co-pyrolysis of sewage sludge (SS) and digested manure (DM) has been investigated. The char yield from the pyrolysis of DM (dry ash free basis) was higher than that from SS, which is consistent with its higher lignin and lower extractive contents. The pyrolysis of SS produced a gas with higher LHV, but the DM char exhibited better characteristics for energetic applications. The organic compounds and water yields (dry ash free basis) were larger in the pyrolysis of SS, which could be due to its higher extractive and protein contents, respectively.

The liquid obtained from the pyrolysis of each residue showed an aqueous phase and an organic phase. The main compounds in the organic phase from SS were carboxylic acids whereas phenols were the main compounds in the organic phase from DM. The aqueous phases from each residue were rich in carboxylic acids, but the aqueous phase from SS also contained amides in large proportions, which explains its higher pH.

The product yields of the co-pyrolysis of SS and DM did not show noticeable

synergistic effects, with the exception of the yields of organic compounds being slightly higher than the predicted average. No remarkable synergistic effects were observed in the liquid phases properties. However, some interactions were detected in the chemical composition of the liquid phases. The proportion of fatty acids decreased and the proportion of aliphatic nitriles increased in the organic phase from the pyrolysis of the SS/DM blend in comparison to the predicted proportions. Finally, no important interactions were found from an energetic point of view. The similar ash contents in SS and DM could explain the small synergistic effect on their co-pyrolysis. Therefore, co-pyrolysis of SS and DM could be a feasible management alternative for these residues in locations where both wastes are generated locally, since the benefits and the drawbacks of the co-pyrolysis are similar to those of the pyrolysis of pure residues.

ACKNOWLEDGEMENTS

The authors would like to acknowledge the use of the Servicio General de Apoyo a la Investigación-SAI and the Instituto de Nanociencia de Aragón (INA), Universidad de Zaragoza. The authors also thank the Centro Tecnológico Agropecuario Cinco Villas for determining protein, lignin, acid detergent fraction and neutral detergent fraction contents in the raw materials. José Antonio Mateo and Olga Marin of I3A are acknowledged for their analytical assistance. The authors would also like to express their gratitude to the Aragon Government and European Social Fund (GPT group) and to MINECO and FEDER (Project CTQ2013-47260-R) for financial support.

REFERENCES

601 Abrego, J., Arauzo, J., Luis Sanchez, J., Gonzalo, A., Cordero, T., Rodriguez-Mirasol, J.,
602 2009. Structural Changes of Sewage Sludge Char during Fixed-Bed Pyrolysis. Ind. Eng.
603 Chem. Res. 48, 3211-3221.
604 Abrego, J., Luis Sanchez, J., Arauzo, J., Fonts, I., Gil-Lalaguna, N., Atienza-Martinez,
605 M., 2013. Technical and Energetic Assessment of a Three-Stage Thermochemical
606 Treatment for Sewage Sludge. Energy Fuels 27, 1026-1034.
607 Agblevor, F.A., Beis, S., Kim, S.S., Tarrant, R., Mante, N.O., 2010. Biocrude oils from
608 the fast pyrolysis of poultry litter and hardwood. Waste Manage. 30, 298-307.
609 Alvarez, J., Amutio, M., Lopez, G., Bilbao, J., Olazar, M., 2015. Fast co-pyrolysis of
610 sewage sludge and lignocellulosic biomass in a conical spouted bed reactor. Fuel 159,
611 810-818.
612 Amen-Chen, C., Pakdel, H., Roy, C., 2001. Production of monomeric phenols by
613 thermochemical conversion of biomass: a review. Bioresour. Technol. 79, 277-299.
614 Atienza-Martinez, M., Francisco Mastral, J., Abrego, J., Ceamanos, J., Gea, G., 2015.
615 Sewage Sludge Torrefaction in an Auger Reactor. Energy Fuels 29, 160-170.
616 Aznar, M., Gonzalez, A.E., Manya, J.J., Sanchez, J.L., Murillo, M.B., 2007.
617 Understanding the effect of the transition period during the air gasification of dried
618 sewage sludge in a fluidized bed reactor. International Journal of Chemical Reactor
619 Engineering 5.
620 Azuara, M., Fonts, I., Barcelona, P., Murillo, M.B., Gea, G., 2013. Study of catalytic post-
621 treatment of the vapours from sewage sludge pyrolysis by means of gamma-Al_2O_3. Fuel
622 107, 113-121.
623 Brown, T.R., Thilakaratne, R., Brown, R.C., Hu, G., 2013. Techno-economic analysis of
624 biomass to transportation fuels and electricity via fast pyrolysis and hydroprocessing.
625 Fuel 106, 463-469.

626 Cao, J.-P., Xiao, X.-B., Zhang, S.-Y., Zhao, X.-Y., Sato, K., Ogawa, Y., Wei, X.-Y.,
627 Takarada, T., 2011. Preparation and characterization of bio-oils from internally
628 circulating fluidized-bed pyrolyses of municipal, livestock, and wood waste. Bioresour.
629 Technol. 102, 2009-2015.
630 Cuetos, M.J., Gomez, X., Martinez, E.J., Fierro, J., Otero, M., 2013. Feasibility of
631 anaerobic co-digestion of poultry blood with maize residues. Bioresour. Technol. 144,
632 513-520.
633 Das, D.D., Schnitzer, M.I., Monreal, C.M., Mayer, P., 2009. Chemical composition of
634 acid–base fractions separated from biooil derived by fast pyrolysis of chicken manure.
635 Bioresour. Technol. 100, 6524-6532.
636 Ding, H.-S., Jiang, H., 2013. Self-heating co-pyrolysis of excessive activated sludge with
637 waste biomass: Energy balance and sludge reduction. Bioresour. Technol. 133, 16-22.
638 Eudy, L.W., Walla, M.D., Hudson, J.R., Morgan, S.L., Fox, A., 1985. Gas
639 chromatography—mass spectrometry studies on the occurrence of acetamide,
640 propionamide, and furfuryl alcohol in pyrolyzates of bacteria, bacterial fractions, and
641 model compounds. J. Anal. Appl. Pyrolysis 7, 231-247.
642 Eurostat, 2014. Sewage sludge production and disposal from urban wastewater treatment
643 plants. http://ec.europa.eu/eurostat/web/products-datasets/-/env_ww_spd (accessed
644 22.07.16).
645 Fonts, I., Gea, G., Azuara, M., Ábrego, J., Arauzo, J., 2012. Sewage sludge pyrolysis for
646 liquid production: A review. Renew. Sust. Energ. Rev. 16, 2781-2805.
647 Fonts, I., Navarro-Puyuelo, A., Ruiz-Gomez, N., Atienza-Martínez, M., Wisniewsky, A.,
648 Gea, G., 2016. Assessment of the Production of Value-Added Chemical Compounds from
649 Sewage Sludge Pyrolysis Liquids. Energy Technol. 4, 1-22.

650 Fullana, A., Conesa, J.A., Font, R., Martin-Gullon, I., 2003. Pyrolysis of sewage sludge:
651 nitrogenated compounds and pretreatment effects. J. Anal. Appl. Pyrolysis 68-9, 561-575.
652 Gil-Lalaguna, N., Sanchez, J.L., Murillo, M.B., Atienza-Martinez, M., Gea, G., 2014.
653 Energetic assessment of air-steam gasification of sewage sludge and of the integration of
654 sewage sludge pyrolysis and air-steam gasification of char. Energy 76, 652-662.
655 Integrated Waste Management Plan of Aragón (Plan GIRA).
656 Jeong, Y.W., Choi, S.K., Choi, Y.S., Kim, S.J., 2015. Production of biocrude-oil from
657 swine manure by fast pyrolysis and analysis of its characteristics. Renew. Energy 79, 14-
658 19.
659 Kebelmann, K., Hornung, A., Karsten, U., Griffiths, G., 2013. Intermediate pyrolysis and
660 product identification by TGA and Py-GC/MS of green microalgae and their extracted
661 protein and lipid components. Biomass Bioenergy 49, 38-48.
662 Li, S., Xu, S., Liu, S., Yang, C., Lu, Q., 2004. Fast pyrolysis of biomass in free-fall reactor
663 for hydrogen-rich gas. Fuel Process. Technol. 85, 1201-1211.
664 Manya, J.J., Sanchez, J.L., Abrego, J., Gonzalo, A., Arauzo, J., 2006. Influence of gas
665 residence time and air ratio on the air gasification of dried sewage sludge in a bubbling
666 fluidised bed. Fuel 85, 2027-2033.
667 Meng, J., Wang, L., Liu, X., Wu, J., Brookes, P.C., Xu, J., 2013. Physicochemical
668 properties of biochar produced from aerobically composted swine manure and its
669 potential use as an environmental amendment. Bioresour. Technol. 142, 641-646.
670 Mullen, C.A., Boateng, A.A., 2011. Production and Analysis of Fast Pyrolysis Oils from
671 Proteinaceous Biomass. Bioenerg. Res. 4, 303-311.
672 Nik-Azar, M., Hajaligol, M.R., Sohrabi, M., Dabir, B., 1997. Mineral matter effects in
673 rapid pyrolysis of beech wood. Fuel Process. Technol. 51, 7-17.

674 Parnaudeau, V., Dignac, M.-F., 2007. The organic matter composition of various
675 wastewater sludges and their neutral detergent fractions as revealed by pyrolysis-GC/MS.
676 J. Anal. Appl. Pyrolysis 78, 140-152.
677 Prins, M.J., Ptasinski, K.J., Janssen, F., 2006. Torrefaction of wood - Part 2. Analysis of
678 products. J. Anal. Appl. Pyrolysis 77, 35-40.
679 Qu, T., Guo, W., Shen, L., Xiao, J., Zhao, K., 2011. Experimental Study of Biomass
680 Pyrolysis Based on Three Major Components: Hemicellulose, Cellulose, and Lignin. Ind.
681 Eng. Chem. Res. 50, 10424-10433.
682 Ro, K.S., Hunt, P.G., Jackson, M.A., Compton, D.L., Yates, S.R., Cantrell, K., Chang,
683 S., 2014. Co-pyrolysis of swine manure with agricultural plastic waste: Laboratory-scale
684 study. Waste Manage. 34, 1520-1528.
685 Samanya, J., Hornung, A., Apfelbacher, A., Vale, P., 2012. Characteristics of the upper
686 phase of bio-oil obtained from co-pyrolysis of sewage sludge with wood, rapeseed and
687 straw. J. Anal. Appl. Pyrolysis 94, 120-125.
688 Sanchez, M.E., Martinez, O., Gomez, X., Moran, A., 2007. Pyrolysis of mixtures of
689 sewage sludge and manure: A comparison of the results obtained in the laboratory (semi-
690 pilot) and in a pilot plant. Waste Manage. 27, 1328-1334.
691 Schnitzer, M.I., Monreal, C.M., Jandl, G., Leinweber, P., Fransham, P.B., 2007. The
692 conversion of chicken manure to biooil by fast pyrolysis II. Analysis of chicken manure,
693 biooils, and char by curie-point pyrolysis-gas chromatography/mass spectrometry (Cp
694 Py-GC/MS). J. Environ. Sci. Health Part B-Pestic. Contam. Agric. Wastes 42, 79-95.
695 Schumacher, B.A., 2002. Methods for the determination of total organic carbon (TOC)
696 in soils and sediments, NCEA-C- 1282 EMASC-001. United States Environmental
697 Protection Agency, Las Vegas.

698 Sekiguchi, Y., Shafizadeh, F., 1984. THE EFFECT OF INORGANIC ADDITIVES ON
699 THE FORMATION, COMPOSITION, AND COMBUSTION OF CELLULOSIC
700 CHAR. Journal of Applied Polymer Science 29, 1267-1286.
701 Smith, K.M., Fowler, G.D., Pullket, S., Graham, N.J.D., 2009. Sewage sludge-based
702 adsorbents: A review of their production, properties and use in water treatment
703 applications. Water Res. 43, 2569-2594.
704 Socrates, G., 2004. Infrared and Raman Characteristic Group Frequencies: Tables and
705 Charts, third ed. John Wiley & Sons, Ltd, Chichester.
706 Subedi, R., Taupe, N., Pelissetti, S., Petruzzelli, L., Bertora, C., Leahy, J.J., Grignani, C.,
707 2016. Greenhouse gas emissions and soil properties following amendment with manure-
708 derived biochars: Influence of pyrolysis temperature and feedstock type. J. Environ.
709 Manage. 166, 73-83.
710 Troy, S.M., Nolan, T., Leahy, J.J., Lawlor, P.G., Healy, M.G., Kwapinski, W., 2013.
711 Effect of sawdust addition and composting of feedstock on renewable energy and biochar
712 production from pyrolysis of anaerobically digested pig manure. Biomass Bioenergy 49,
713 1-9.
714 Tsuge, S., Matsubara, H., 1985. High-resolution pyrolysis-gas chromatography of
715 proteins and related materials. J. Anal. Appl. Pyrolysis 8, 49-64.
716 Wright, M.M., Daugaard, D.E., Satrio, J.A., Brown, R.C., 2010. Techno-economic
717 analysis of biomass fast pyrolysis to transportation fuels. Fuel 89, Supplement 1, S2-S10.
718 Zabeti, M., Nguyen, T.S., Lefferts, L., Heeres, H.J., Seshan, K., 2012. In situ catalytic
719 pyrolysis of lignocellulose using alkali-modified amorphous silica alumina. Bioresour.
720 Technol. 118, 374-381.

721 Zhang, J., Tian, Y., Cui, Y., Zuo, W., Tan, T., 2013. Key intermediates in nitrogen
722 transformation during microwave pyrolysis of sewage sludge: A protein model compound
723 study. Bioresour. Technol. 132, 57-63.
724 Zhang, W., Yuan, C., Xu, J., Yang, X., 2015. Beneficial synergetic effect on gas
725 production during co-pyrolysis of sewage sludge and biomass in a vacuum reactor.
726 Bioresour. Technol. 183, 255-258.
727 Zuo, W., Jin, B., Huang, Y., Sun, Y., 2014. Characterization of top phase oil obtained
728 from co-pyrolysis of sewage sludge and poplar sawdust. Environ. Sci. Pollut. Res. 21,
729 9717-9726.

730